JCTC Journal of Chemical Theory and Computation

Article

pubs.acs.org/JCTC

On the N_1−H and N_3−H Bond Dissociation in Uracil by Low Energy Electrons: A CASSCF/CASPT2 Study

Israel González-Ramírez,[†] Javier Segarra-Martí,[†] Luis Serrano-Andrés,[†] Manuela Merchán,[†] Mercedes Rubio,*[,†] and Daniel Roca-Sanjuán*[,‡]

[†]Instituto de Ciencia Molecular, Universitat de València, P.O. Box 22085, 46071 València, Spain

[‡]Department of Chemistry−Ångström, Theoretical Chemistry Program, Uppsala Univeristy, P.O. Box 518, 75120 Uppsala, Sweden

Supporting Information

ABSTRACT: The dissociative electron-attachment (DEA) phenomena at the N_1−H and N_3−H bonds observed experimentally at low energies (<3 eV) in uracil are studied with the CASSCF/CASPT2 methodology. Two valence-bound π^- and two dissociative σ^- states of the uracil anionic species, together with the ground state of the neutral molecule, are proven to contribute to the shapes appearing in the experimental DEA cross sections. Conical intersections (CI) between the π^- and σ^- are established as the structures which activate the DEA processes. The N_1−H and N_3−H DEA mechanisms in uracil are described, and experimental observations are interpreted on the basis of two factors: (1) the relative energy of the $(U-H)^-$ + H fragments obtained after DEA with respect to the ground-state equilibrium structure (S_0) of the neutral molecule (threshold for DEA) and (2) the relative energy of the CIs also with respect to S_0 (band maxima). The π_1^- state is found to be mainly responsible for the N_1−H bond breaking, whereas the π_2^- state is proved to be involved in the cleavage of the N_3−H bond.

INTRODUCTION

Irradiation of nucleic acids can cause damage in several ways.[1,2] When cellular DNA/RNA is ultraviolet (UV) irradiated, the formation of lesions among adjacent pyrimidine bases (namely cyclobutane pyrimidine dimers) is the most frequent route of damage.[3,4] Nonetheless, other reactive pathways are available in DNA/RNA that take place primarily through secondary reactions involving species generated within the complex cellular system in an initial ionization step (electrons, OH, H, DNA/RNA radicals).[2] These events mostly remove electrons either from the molecules' valence orbitals in chemical bonds or from the inner core of individual atoms, subsequently causing structural lesions.[5] The remarkable work of Boudaiffa et al. unveiled the fact that low energy (3−20 eV) electron attachment in thin films of DNA could lead, through decay of temporary anion states, to single and double strand break.[6] Furthermore, data from the international commission on radiation units and measurements[7] have shown that these electrons (3−20 eV) lose the kinetic energy within picoseconds through collisions, and yet it is possible for electrons in the energy range 0.1−3 eV to cause dissociations in DNA/RNA.[5,8] Excited states of the temporary anions involving π^* electrons of the nucleobase and σ^* electrons of the sugar−phosphate C−O bond have been shown to be relevant in the mechanism of DNA strand cleavage.[2,9,10]

Nucleobases themselves can undergo decomposition reactions after attachment of low-energy electrons.[11] The most efficient reactive process in the gas phase implies the dissociative electron attachment (DEA) of the temporary anionic base which dissociates into the $(nucleobase-H)^-$ ion plus a hydrogen atom. The DEA in uracil at subexcitation energies (<3 eV) has been observed in several experiments.[5,12−17] Measurements of the total yield of $(U-H)^-$ ion as a function of electron energy show a first peak at 0.69 eV, followed by a strong and sharp feature at 1.01 eV, and next a broad band with a maximum around 1.7 eV. On the basis of theoretical G2MP2[13,17] and P2MP2[5] calculations of the dissociation energies (D) for the N−H and C−H bonds of the neutral uracil molecule and the electron affinity (EA) of the radical formed by the loss of H from the particular site, the DEA values at the N−H positions were established at low energies. In particular, the thresholds for H abstraction (E) were obtained at 0.8, 1.4, 2.2, and 2.7 eV at the N_1, N_3, C_6, and C_5 sites, respectively ($E = D - EA$)[13,17,5] (see atom labeling in Figure 1). Regarding the energy range for the different N−H

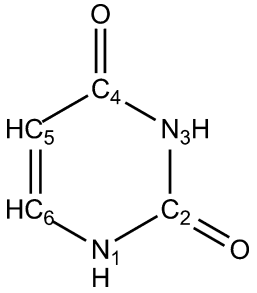

Figure 1. Numbering and atom labeling for uracil.

DEA, Ptasinska et al. measured the yields of $(U-H)^-$ production in the canonical uracil and the methylated derivative 3-methyluracil, concluding that the N_3−H channel is only responsible for the feature in the spectrum at energies above 1.4 eV, whereas the N_1−H channel is accessible also at lower energies.[17] Both theoretical and experimental results clearly

Received: February 21, 2012
Published: July 12, 2012

   dx.doi.org/10.1021/ct300153f | J. Chem. Theory Comput. 2012, 8, 2769−2776

indicate that the two lowest peaks in the DEA experiments correspond to the N_1−H bond dissociation.

The nature of the anions involved in the mentioned DEA processes is more difficult to determine. Polar molecular systems can trap electrons in their long-range dipole field if they possess a dipole moment greater than about 2.5 D.[18−21] Such large polarity becomes a challenge both theoretically and experimentally for the correct determination of the EA[22] and the study of the low energy electron attachment behavior in a nucleic acid base such as uracil with a dipole moment of about 4.3 D.[18] The dilemma arises when this great polarity allows the existence of two different types of anions, dipole-bound (DB) and valence-bound (VB), which are expected to share the same energy region.[18,22] According to previous theoretical calculations, the vertical EA of the VB uracil anion is negative (VEA = −0.61 eV) and becomes very close to zero after vibrational relaxation (the adiabatic EA is −0.01 eV),[22] whereas the DB anion has an attractive electrostatic interaction between the electron and the molecule (EA = 0.085 eV).[18] Since the uracil nucleobase does not stabilize an electron in the valence shell, the relevance of the DB anion in the chemistry of the nucleobase is enhanced. Taking into account the coexistence of both DB and VB anions in the same range of energies and the fact that the lowest π anion appears in the electron transmission spectroscopy (ETS) data at lower energies than the threshold for the N−H DEA,[8,16] Burrow and co-workers[14−16] and Gallup et al.[23] focused on the DB anion in order to interpret the lowest two DEA signals measured in the experiments. The ETS technique, however, underestimates the energies of the anion, as shown by more recent high-level ab initio computations.[22] In the studies from Burrow and co-workers,[14−16] two-state configuration interaction calculations based on two restricted open-shell Hartree−Fock wave functions representing the DB and σ^- states were performed at different N−H distances.[15] The energies obtained, together with various empirical quantities, were then employed to build the Morse-based potential energy curves (PECs) and later to estimate the DEA signals. The peaks at 0.69 and 1.01 eV were attributed in such manner to vibrational Feshbach resonances (VFRs) of the DB anion state with vibrational levels ν = 2 and 3, respectively. Gallup et al. combined recently the finite element discrete model with the resonance *R*-matrix theory to calculate the positions of the VFRs, which were found 0.1−0.2 eV higher as compared to the experiments.[23] On the other hand, the broad band in the experimental DEA cross-section was supposed to be caused by the π_2^- VB anion,[14−16,23] according to the ETS results.[8] However, no clear evidence of this fact was provided.

The VB anion of uracil is more relevant in condensed phases, where DB anions are likely to be absent.[24−26] Although most experiments have been performed in the gas phase, there is evidence of hydrogen loss in other phases such as superfluid helium droplets kept at low temperatures[27] or even condensed-phase DNA.[28] Li et al. computed the VB DEA energy threshold for the N−H and C−H bonds in uracil with the DFT and CBS-Q methods.[29] The authors also calculated the PEC of the ground state of the anion along the N−H and C−H bonds at the DFT level. In agreement with other computations at the G2MP2 and P2MP2 levels,[5,13,17] the energy trend obtained for DEA at the N−H and C−H sites was N1 < N3 < C6 < C5.[29] In these studies, the lowest VB anion was considered as the responsible species for all the N−H and C−H DEA processes. Along the PECs, the π anion state was shown to evolve toward a σ state localized in the particular bond that dissociates. The single-reference methods employed by Li et al. did not permit them to study the role of excited states of the anion, such as the π_2^-, or to analyze properly the mixing of the π^- and σ^- states. The authors suggested further investigations able to describe the section of the PECs where states cross.

The present work is aimed to study, for the first time by means of the CASSCF/CASPT2 method,[33−36] the hydrogen dissociation process (DEA) that takes place in the uracil nucleobase at the N_1−H and N_3−H sites as a result of adding a low-energy electron into an empty π^* orbital. The role of the ground as well as the low-lying excited states of the anion in both N−H dissociations is intended. Conical intersections (CIs) between the PECs of the $\pi^-$and σ^-states along the N−H reactive coordinates will be interpreted as the points on the PECs which activate the hydrogen loss processes in the subsequent events that follow the electron attachment in the uracil nucleobase. Such crossing points have been found to be relevant features in the mechanism of several photochemical phenomena in organic molecules.

METHODS AND COMPUTATIONAL DETAILS

Characterization of the lowest-lying valence states of the uracil anion and the ground state of the uracil neutral molecule along the N_1−H and N_3−H reactive coordinates is performed in the present study at the CASSCF/CASPT2 level of theory to establish the mechanism for hydrogen loss caused by electron-attachment. Previous benchmark calculations on the determination of the vertical and adiabatic EAs of DNA/RNA nucleobases were considered here to select the most appropriate methodology.[22] These benchmark reference values lead to the characterization of the ground state of the valence anion of uracil as a temporary anion state (resonance), in line with the ETS data, since its energy is higher (vertical and adiabatically) than the energy of the ground state of the neutral molecule and consequently it is unstable with respect to electron detachment.[30] The excited states of the uracil anion have accordingly the same characteristic. Temporary anion states are difficult to treat using conventional quantum chemistry techniques since calculations can tend to put the extra electron into the most diffuse orbital available in order to simulate the neutral molecule plus a free electron. Despite the difficulties, it is also possible to obtain reliable solutions representing the resonance states.[22] It was shown in previous studies of biphenyl and *p*-benzosemiquinone radical anions[31,32] that the CASSCF method is able to provide well-localized solutions which can be regarded as a discrete representation of the temporary anion states. Spurious solutions where the extra electron is located far from the molecule in a diffuse orbital can also appear and are not reliable. To distinguish between both types of solutions, in addition to the analysis of the natural orbital with the unpaired electron, we have determined the spatial extension of the electron density ($\langle r^2 \rangle$) by means of the trace of the second Cartesian moment tensor. Valence localized anionic states have spatial extensions slightly larger than the neutral system, whereas clear differences appear for diffuse states (or mixed valence dipole-bound states).

The basis set of atomic natural orbital, ANO-L type, contracted to C, N, O [4s3p1d]/H [2s1p] (hereafter, ANO-L 431/21) was chosen as a compromise between accuracy and computational cost.[22] No symmetry requirements (C_1 symmetry) were employed in the computations. The geometries of the neutral and the hydrogen dissociated $(U-H_1)^-$ and $(U-H_3)^-$ uracil anionic systems were optimized at the

CASSCF level using an active space comprising the whole valence π system of the nucleobase, that is, 10 electrons distributed among 8 π molecular orbitals, namely CASSCF(10,8). Planar geometries were obtained for these anions. The zero-point vibrational energy correction (ZPVE) was calculated in these minima at the same level of theory with the harmonic approximation. A larger active space was used within the CASSCF method for the computations of the PECs along the N−H reactive coordinates, including 4 additional orbitals: the σ^* orbitals related to the N_1−H and N_3−H bonds plus 2 additional diffuse orbitals required to stabilize the active space along the PECs. In total, there are 11 active electrons and 12 active orbitals [hereafter, CASSCF(11,12)]. The shape of the most relevant natural orbitals can be found in Figure S1. Eight states were averaged with equal weights within the CASSCF method for the PECs of the uracil anion.

Several computational strategies were employed as required in order to determine the relevant PEC features to the DEA processes which occur at the N−H sites. (1) The PECs between the neutral structure and the two $(U-H)^-$ anions were explored initially by means of the linear interpolation of internal coordinates (LIIC) procedure. This method allows the location of the crossing points between the PECs of the low-lying states of the anion which mediates the hydrogen loss phenomenon. The final hydrogen separation from the uracil molecular frame in the LIIC was set at 3.0 Å. (2) A constrained optimization with fixed N_3−H bond length was also performed at the CASSCF(11,12) level to analyze the role of the π_2^- anionic state in the DEA events. The geometry of the π_2^- state was optimized with fixed N_3−H values corresponding to the first point of the LIIC curve (the ground-state equilibrium geometry of the uracil neutral molecule). All other degrees of freedom of the uracil molecule are allowed to relax. (3) CASSCF(11,12) minimum energy path (MEP) computations on the PEC of the π_2^- excited state of the uracil anion from the equilibrium geometry of the neutral system were carried out to describe both the evolution of this state after electron attachment and the crossing with the dissociative σ^- excited state which ends in the fragmented nucleobase $[(U-H)^- + H]$. MEPs were built as steepest descendent paths,[37,38] in which each step implies the minimization of the energy on a hyperspherical cross section of the PEC centered on the initial geometry within a predefined radius of 0.09 au. Mass-weighted coordinates were used. Test MEP calculations were also carried out with a smaller hyperspherical radius of 0.05 au and gradients computed at the CASSCF level with a small active space comprising 7 electrons distributed among 9 orbitals. Two occupied and one virtual π natural orbitals, with occupation numbers close to two and zero, respectively, were excluded from the active space.

The CASPT2 method was employed at the geometries obtained in the LIIC, constrained optimizations, and MEPs to obtain the dynamic correlation for the ground state of the neutral uracil and the low-lying doublet states of the anionic system. In order to minimize weakly interacting intruder states, the imaginary level-shift technique with a parameter of 0.2 au was employed.[39] The IPEA definition of the zeroth-order Hamiltonian in the CASPT2 method, with a value of 0.25 au, was found previously to improve the results of EA in nucleobases and consequently was employed here.[22]

All the calculations were performed with the CASSCF/CASPT2 method as implemented in the versions 7 of the MOLCAS quantum-chemistry package of software.[40,41]

RESULTS AND DISCUSSION

During the electron attachment process in the uracil molecule, the system is initially ionized to one of the low-lying states of the anion producing a temporary anionic state with the geometry of the neutral molecule (Franck−Condon transition). This state must evolve toward a dissociative σ^- state localized in the N−H bonds in order to produce the DEA phenomenon, through a crossing region between the curves of the initial π^- and final σ^- states. The latter anionic state will drive the molecule to the separated hydrogen and $(U-H)^-$ fragments. Several theoretical magnitudes are valuable to describe the mechanism for DEA and to interpret the experimental observations: the vertical electron affinity (VEA) of the neutral uracil at the ground-state equilibrium structure, the relative energies between the neutral nucleobase plus the incident electron (reactants) and the H atom plus the $(U-H)^-$ ion (products), and the crossing regions which activate the DEA phenomenon. The corresponding CASSCF/CASPT2 data will be presented and discussed in the following sections.

Vertical Electron Affinities of the Uracil Neutral System. Table 1 compiles the present computed CASPT2 VEAs for the five low-lying states of the anion at the geometry of the neutral system, together with the related data measured in ETS experiments[8] and reference values from a previous work.[22] The results obtained here for the lowest-lying VEA are in agreement with the data computed at higher levels of theory. Systematic differences are found between all the theoretical VEAs and the vertical attachment energies measured in ETS experiments. Such discrepancies were carefully analyzed in the previous study on the accurate determination of the EAs in nucleobases.[22] The authors concluded that the ETS technique underestimates the relative energy of the anion states with respect to the neutral molecule by near 0.3−0.4 eV in nucleobases, which is in agreement with other studies.[42]

Table 1. Experimental Data Derived from Electron Transmission Spectroscopy (ETS) and Theoretical Vertical Electron Affinities (eV) for the Low-Lying Anionic States in Uracil

anion state	CASPT2//CASSCF ANO-L 431/21[a]	CASPT2//CASSCF ANO-L 4321/321[b]	CCSD(T)//CCSD aug-cc-pVDZ[b]	exp ETS[c]
π_1^-	−0.69	−0.61	−0.64	−0.22
$diff_{N1H}^-$	−0.84			
$diff^-$	−1.69			
$diff_{N3H}^-$	−1.74			
π_2^-	−2.24			−1.58

[a]This work. [b]Reference 22. [c]Reference 8.

The present VEAs show that the lowest VB-anionic state has π character and three diffuse states are located between the π_1^- and π_2^- states. As shall be seen below, two of these diffuse states ($diff_{N1H}^-$ and $diff_{N3H}^-$) are connected to the dissociative anionic states in which the electron occupies the σ^* orbitals of the N_1−H and N_3−H bonds, respectively. However, at the equilibrium geometry of the neutral uracil, these solutions correspond to diffuse or mixed valence and dipole-bound states and the VEA cannot be considered as reliable. The spatial extensions $\langle r^2 \rangle$ of these states are 177, 184, and 172 au^2, for $diff_{N1H}^-$, $diff^-$, and $diff_{N3H}^-$, respectively, which are clearly much larger than the results obtained for the valence localized π_1^-

and π_2^- anionic states and neutral S_0 ground state at this geometry, with values in the range 106−128 au^2.

Energy Thresholds for the Reaction U + e$^-$ → (U−H)$^-$ + H. The energy difference (E) between products and reactants of the DEA reaction has been estimated in the literature at different levels of theory by using the bond dissociation energy of the neutral uracil [D(N−H)] and the EA of the radical formed after H loss from the particular site [EA(N−H)], through the equation $E = D - EA$,[5,13,17,29] where E stands for the energy threshold of the reaction. Table 2 compiles the results obtained by Märk and co-workers with the P2MP2[5] and G2MP2[13,17] methods, data from Li et al.[29] with the DFT and CBS-Q methods, and the present computed CASPT2 values. The theoretical results establish the threshold for N_1−H and N_3−H DEA at 0.6−0.8 and 1.2−1.4 eV, respectively. Such energies correspond to the lowest band and the origin of the broad band in the DEA cross sections.[5] These thresholds, therefore, allow an estimate of the regions in the experimental spectrum related to each one of the N−H dissociation processes. While energies below 1.2−1.4 eV are sufficient to break the N_1−H bond, higher energies are needed for the N_3−H cleavage. The same conclusions were obtained from experiments with methylated uracil and thymine nucleobases at the N_1 and N_3 positions,[17] where the activation of the dissociative N_1−H path was exclusively achieved at energies below the calculated 1.4 eV threshold, whereas at energies above that value, dissociation at the N_3−H site became accessible.

Table 2. Dissociation Energies (in eV) Corresponding to the N_1−H and N_3−H Bonds Computed at Different Levels of Theory with Zero-Point Vibrational Energies Included at the Same Level of Theory

	P2MP2[a]	G2MP2[b]	DFT[c]	CBS-Q[c]	CASPT2[d]
N_1H	0.8	0.8	0.71	0.84	0.61
N_3H	1.4	1.4	1.25	1.36	1.21

[a]Reference 5. [b]References 13, 17. [c]Reference 29. [d]This work.

Potential Energy Curves along the N−H Reactive Coordinates. The mapping of the PECs for the ground state of the neutral uracil molecule and the low-lying VB anionic states of the anion system was performed at the CASPT2 level from the Franck−Condon region at the ground-state equilibrium structure of the neutral nucleobase and along the reactive coordinates which lead to the U−H_1 and U−H_3 species. Figures 2 and 3 display the results obtained for the N_1−H and N_3−H DEA processes, respectively. Four anionic states are represented in the figures: the lowest-lying π_1^- and π_2^- VB states and the dissociative σ^- states. In the π_1^- and π_2^- states the attached electron is placed in a valence π orbital, whereas the antibonding σ^* orbital of the N_1−H and N_3−H bonds is occupied in the σ-like type states of the anion. In agreement with Li et al.,[29] the DEA channel in which the N_1−H is dissociated appears at lower energies with respect to the N_3−H. The σ^- states have intrinsic dissociative character, although it is not clear from Figures 2 and 3. The reasons are related to the mixed valence and dipole-bound solutions found for these states in the Franck−Condon region which cause an underestimation of the energies. In Figure 2, the σ_{N1H}^- state shows initially spatial extensions, $\langle r^2 \rangle$, around 172 au^2 (dashed line), becoming localized at larger N_1−H distances with an average $\langle r^2 \rangle$ of 138 au^2. This latter value is close to the result found for the dissociated anion (133 au^2), which is a stable anion (positive EA), and also close to the $\langle r^2 \rangle$ extensions computed for the π_1^- (128−134 au^2), π_2^- (124−125 au^2), and S_0 (95−111 au^2) states. In Figure 3, similar findings are obtained. The first points of the σ_{N3H}^- state have $\langle r^2 \rangle$ around 169 au^2, and next, the electron becomes localized in the valence space, with an averaged $\langle r^2 \rangle$ value of 129 au^2, in line with the results obtained for the dissociated anion and the π_1^-, π_2^-, and S_0 states (126, 126−133, 124−125, and 105−109 au^2, respectively). Hence, descriptions on the starting region of the σ_{N1H}^- and σ_{N3H}^- states with the employed methodology are only approximate, whereas the points at larger N−H bond lengths and the π_1^- and π_2^- anion states are accurately determined.

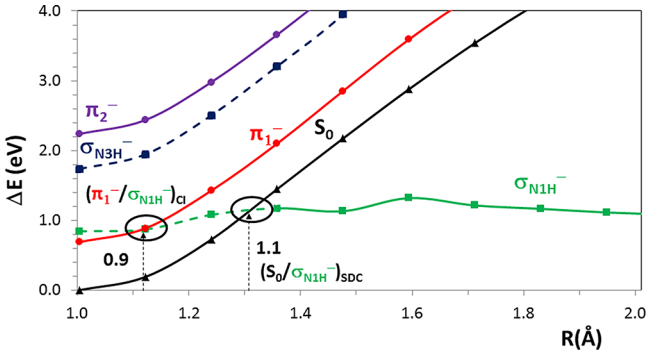

Figure 2. CASPT2 potential energy curves (PECs) for the ground state of the uracil neutral molecule (S_0) and the π_1^-, π_2^-, σ_{N1H}^-, and σ_{N3H}^- states of the anionic species along the N_1−H reactive coordinate. Dashed lines indicate points with mixed valence and dipole-bound states (see text). The corresponding CASSCF PECs can be found in Figure S2.

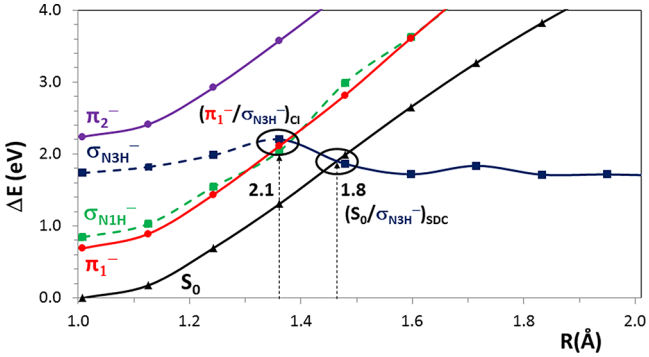

Figure 3. CASPT2 potential energy curves (PECs) for the ground state of the uracil neutral molecule (S_0) and the π_1^-, π_2^-, σ_{N1H}^-, and σ_{N3H}^- states of the anionic species along the N_3−H reactive coordinate. Dashed lines indicate points with mixed valence and dipole-bound states (see text). The corresponding CASSCF PECs can be found in Figure S3.

Two types of crossings can be distinguished in Figures 2 and 3, which are responsible for the activation of the hydrogen loss phenomena: (1) CIs between the π^- and σ^- states and (2) singlet−doublet crossings (SDCs) between the ground state of the neutral system and the σ^- states of the anion. While the role of the first crossing points in modern photochemistry is widely recognized, SDCs are not so well-known. In such SDC regions, there exists an energy resonance between the anion and the neutral system plus the electron at infinite distance from the molecular frame. Hence, conversions between both situations are energetically possible. SDCs were suggested in previous

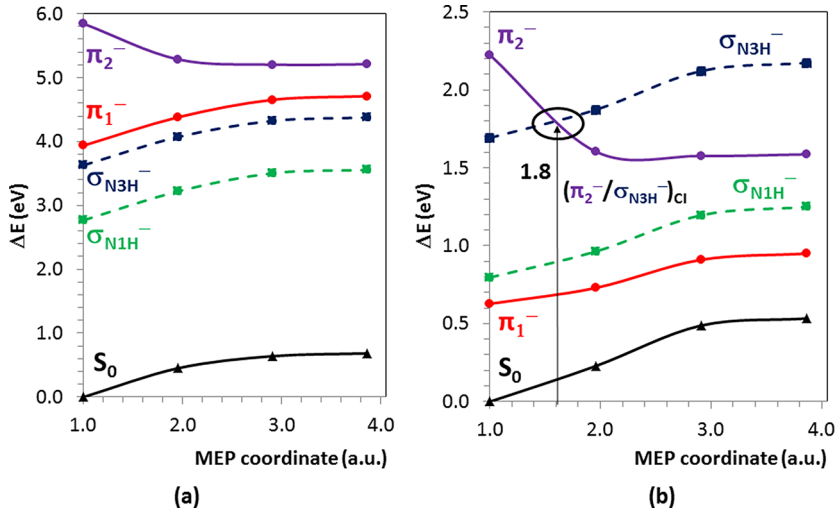

Figure 4. CASSCF (a) and CASPT2 (b) energies for the ground state of the uracil neutral molecule (S_0) and the π_1^-, π_2^-, σ_{N1H}^-, and σ_{N3H}^- states of the anionic species along the minimum energy path (MEP) of the π_2^- state. Dashed lines indicate points with valence and dipole-bound mixing (see text).

works as relevant structures to the charge transport phenomena in DNA/RNA.[43−45]

Figure 2 displays two PEC crossings involving the σ_{N1H}^- state of the anion: $(\pi_1^-/\sigma_{N1H}^-)_{CI}$ and $(S_0/\sigma_{N1H}^-)_{SDC}$. The $(\pi_1^-/\sigma_{N1H}^-)_{CI}$ connects the π_1^- state initially populated after electron-attachment with the state that drives the system toward the fragmented uracil anion $[(U-H_1)^- + H]$. Such structure, $(\pi_1^-/\sigma_{N1H}^-)_{CI}$, has an energy of 0.9 eV and therefore might mediate the DEA process at energies below 1 eV. Two points must be considered here: (1) the diffuse nature of the solutions of the σ_{N1H}^- state at this region avoids an accurate determination of the crossing points, which are expected higher in energy taking into account the dissociative nature of the σ^- states, and (2) tunneling effects will be important in this process as discussed by Scheer et al.,[15] and will operate in the other direction, decreasing the barrier to reach the σ_{N1H}^- state. The approximate $(S_0/\sigma_{N1H}^-)_{SDC}$ point appears around 1.1 eV. Apart from the relevance of such SDC in the DEA phenomenon, the energy of this point can be used as an estimate of the CI between the DB and the σ_{N1H}^- anion states. In fact, the electron is placed far from the molecule in these DB anions, and an attractive electrostatic interaction exists between both fragments; the EA of the DB anion in uracil is 0.085 eV.[18] Therefore, the equilibrium geometries of the DB anions and the neutral system are similar, and the corresponding PECs are close in energy, as explained by Probst et al.[11] In addition, the dipole moment of uracil is not changing significantly along the PEC toward the SDC region; a range of 4.2−4.7 D is obtained for the dipole moment of the neutral molecule among the first four points. Hence, the PEC for the DB anion is expected to be less than 0.1 eV far from the S_0 state (the canonical nucleobases, for example, with a large range of dipole moments of 2.56−6.55 D,[46] have small dipole-bound EAs in all the cases lower than 0.1 eV).[47] Accurate treatments of DB states require very time-demanding approaches[18] which are out of the scope of this work.

A sharp peak at 1.01 eV is observed in the cross sections measured in the DEA experiments, in contrast to the other bands which show less intense and broader features. Gallup and co-workers interpreted the shapes in the spectrum at 0.69 and 1.01 eV as VFRs of the DB anion with vibrational levels $\nu = 2$ and 3, respectively.[14−16,23] On the basis of our findings, which are in agreement with the investigations reported by Li et al.,[29] we set an alert to the conclusions obtained by the former authors:[14−16] the lowest VB π^- anion can also participate in the lowest peaks, in addition to the DB anion. The CI is interpreted in the present study as the point activating the DEA process. The SDC might also be relevant. In addition, assuming that the actual PEC of the DB-anionic state behaves approximately parallel to that related to the neutral (S_0), the DB-like state seems to activate the DEA process at similar energies than the VB π_1^- anion (see Figure 2). An accurate assignment of the peaks at 0.69 and 1.01 eV is not possible at the present because of the intrinsic limitations of the computational strategies employed. Nevertheless, a clear conclusion is obtained: not only the DB anion but also the VB π_1^- anion are responsible for the DEA processes at energies below and around 1 eV.

The CASSCF/CASPT2 results obtained for the PECs along the N_3−H reaction coordinate show also crossings between the π_1^- and S_0 states with the σ_{N3H}^- state (see Figure 3). The approximate energies obtained for these structures are around 2 eV, which locates the related processes in the broad band region of the spectrum. Hence, the electron attached in the π_1^- orbital can also undergo the cleavage of the N_3−H bond, in addition to the participation of the π_1^- state in the DEA reaction at the N_1−H site. Li et al. found similar conclusions by means of DFT constrained optimizations between the ground-state equilibrium structure of this state and the dissociated $(U-H_3)^-$ plus H products.[29] In contrast, on the basis of ETS measurements,[8] Burrow and co-workers[14−16] suggested the π_2^- state as responsible for the broad band in the spectrum, with maximum at 1.7 eV, being the vertical electron attachment energy of the second anionic state measured at −1.58 eV (see Table 1). Similar to the dissociation of the N_1−H bond, a contribution of the DB anion can be expected also here, not suggested previously. The dipole moment of the neutral system changes only slightly (3.7−4.2 D) between the Franck−Condon and the SDC crossing point; therefore, the PECs of the DB anion and the S_0 can be estimated parallel and within an energy separation of 0.1 eV, as in the equilibrium structure of the neutral uracil (0.085 eV).[18]

dx.doi.org/10.1021/ct300153f | J. Chem. Theory Comput. 2012, 8, 2769−2776

Figure 3 shows that the PECs of the π_2^- and σ_{N3H}^- states are indeed relatively close around the Franck−Condon region. Considering the aforementioned underestimation of the σ_{N3H}^- state in these points, both states might cross in the surroundings. A constrained optimization of the π_2^- state with a fixed N_3−H bond distance of 1.00 Å gives rise to an inversion of the PECs, bringing the π_2^- state below the energy of the σ_{N3H}^- state by 0.4 eV at the CASPT2 level. In any case, since the VEA of the π_2^- state is higher than the threshold for DEA at the N_3−H bond, unlike the situation found for the π_1^- state and the N_1−H bond, the initial evolution of the π_2^- state after electron attachment will be important to establish the thresholds for any contribution of this state to the DEA processes. Therefore, we carried out MEP calculations on the π_2^- PEC from the Franck−Condon structure. Figure 4 displays the CASSCF and CASPT2 energies for the relevant neutral and anionic states of uracil in the DEA process along the MEP. The uracil molecule suffers out-of-plane distortions, reaching an equilibrium structure of the π_2^- state with ring-puckering at the end of the MEP. This point, with an energy of 1.59 eV, is obviously the lowest energy structure of the π_2^- anion state, and therefore, no possible contributions to the DEA process can take place from this state at lower energies. Regarding the mixing between the states, at the CASSCF level the π_2^- state is still higher in energy than the σ^- states and no crossings are present along the path. However, the dynamical correlation does not contribute with the same value to the π^- and σ^- states (strong differential correlation effects), and the scenario is completely different at the CASPT2 level. A CI point appears now between the π_2^- and σ_{N3H}^- states, $(\pi_2^-/\sigma_{N3H}^-)_{CI}$, which is the structure responsible for funneling of the system toward the dissociation of the N_3−H bond (cf. Figure 4b). The equilibrium structure of the π_2^- state is only 0.2 eV below $(\pi_2^-/\sigma_{N3H}^-)_{CI}$, although the results for the crossing should be taken with caution due to the difficulties of the method to properly describe the σ^- state. Both the C═O as well as the N_1−C_2 and C_4−C_5 bonds are elongated in the region of the crossing point, as expected due to the antibonding character of the π_2^* orbital at those sites (see Figure S1). But the structure is still planar, and the N_3−H bond length is close to the Franck−Condon geometry. The N_3−H elongation will be driven by the σ_{N3H}^- dissociative state which is populated via the $(\pi_2^-/\sigma_{N3H}^-)_{CI}$. A more restrictive MEP calculation, with a shorter hyperspherical radius (0.05 au), was performed obtaining the same conclusions (cf. Figures S4 and S5). Taking into account the VEA of the π_2^- anion state (2.24 eV), the energy for its equilibrium structure (1.59 eV), and the $(\pi_2^-/\sigma_{N3H}^-)_{CI}$ crossing which activate the DEA mechanism (above 1.8 eV), the region of the broad band maximum in the cross sections of the DEA experiments (around 1.8−2 eV) can be mainly ascribed to the π_2^- state. The π_1^- state might also contribute to this band and the DEA process at the N_3−H site, although a lower-energy dissociative route is possible for such state, involving the N_1−H bond breaking. Therefore, the N_1−H DEA will be the main reactive path driven by the π_1^- state, whereas the π_2^- state can only participate in the N_3−H DEA.

CONCLUSIONS

The CASSCF/CASPT2 method, together with different computational strategies (LIIC, constrained optimizations, and MEPs), has been applied to determine the mechanisms for DEA at the N_1−H and N_3−H sites of uracil involving VB anions. Several low-lying states of the anionic species, with π^- and σ^- character, have been studied. According to the findings obtained and other theoretical results from the literature,[5,13,17,29] the energy threshold for the dissociation of the N_1−H and N_3−H bonds is 0.6−0.8 and 1.2−1.4 eV, respectively, which agrees with the experimental observations. Regarding the mechanism for the DEA phenomena, once the low-energy electron becomes attached into an empty π^* orbital within the uracil monomer, crossing points between the PECs of the π^- and the σ^- states appear at energies around the maxima of the lowest peak and the broad band in the DEA cross sections. The corresponding conical intersections (CIs) can be interpreted as the points which activate the internal conversion to the dissociative σ^- states, therefore driving the system toward the $(U-H)^-$ ion plus a H atom. The π_1^- state is mainly involved in the cleavage of the N_1−H bond, since it crosses the σ_{N1H}^- state at 0.9 eV. Still, it can participate in the N_3−H DEA via a second CI, $(\pi_1^-/\sigma_{N3H}^-)_{CI}$, in the region of the broad band, around 2 eV. The π_2^- state is predicted, however, as the main state responsible for this shape having a crossing point with the σ_{N3H}^- state, $(\pi_2^-/\sigma_{N3H}^-)_{CI}$, in this region.

The present findings complement previous studies focused on the role of the DB states in the DEA phenomena.[14−16] The lowest peak and the sharp shape at 1 eV in the DEA cross section were assigned in those investigations to VFRs of the DB anion with ν = 2 and 3, respectively. The π_2^- was suggested to be involved in the broad band at higher energies. On the basis of our present study, the VB anion of uracil is predicted to be also responsible for the shapes at the lower region of the spectrum, and more insights are provided on the correspondence between the π_2^- state and the broad band.

ASSOCIATED CONTENT

Supporting Information

Additional figures and tables. This material is available free of charge via the Internet at http://pubs.acs.org.

AUTHOR INFORMATION

Corresponding Author

*E-mail: Mercedes.Rubio@uv.es (M.R.), Daniel.Roca@kvac.uu.se (D.R.-S.).

Notes

The authors declare no competing financial interest.

ACKNOWLEDGMENTS

In memory of Luis Serrano-Andrés, who was an excellent scientist, mentor, and friend. Research supported by projects CTQ2010-14892 of the MICINN, the Consolider-Ingenio in Molecular Nanoscience of the Spanish MEC/FEDER CSD2007-0010, and the Generalitat Valenciana. It has also received funding from the European Research Council under the European Community's Seventh Framework Programme (FP7/2007-2013)/ERC grant agreement 255363.

REFERENCES

(1) Connell, P.; Kron, S. J.; Weichselbaum, R. R. Relevance and Irrelevance of DNA Damage Response to Radiotherapy. *DNA Repair* **2004**, *3*, 1245−1251.

(2) Simons, J. How Do Low-Energy (0.1−2 eV) Electrons Cause DNA-Strand Breaks? *Acc. Chem. Res.* **2006**, *39*, 772−779.

(3) Cadet, J.; Vigny, P. The Photochemistry of Nucleic Acids. In *Bioorganic Photochemistry*, 1st ed.; Morrison, H., Ed.; John Wiley & Sons: New York, 1990; Vol. *1*, pp 1−273.

(4) Roca-Sanjuán, D.; Olaso-González, G.; González Ramírez, I.; Serrano-Andrés, L.; Merchán, M. Molecular Basis of DNA Photodimerization: Intrinsic Production of Cyclobutane Cytosine Dimers. *J. Am. Chem. Soc.* **2008**, *130*, 10768−10779.
(5) Hanel, G.; Gstir, B.; Denifl, S.; Scheier, P.; Probst, M.; Farizon, B.; Farizon, M.; Illenberger, E.; Märk, T. D. Electron Attachment to Uracil: Effective Destruction at Subexcitation Energies. *Phys. Rev. Lett.* **2003**, *90*, 188104−188107.
(6) Boudaiffa, B.; Cloutier, P.; Hunting, D.; Huels, M. A.; Sanche, L. Resonant Formation of DNA Strand Breaks by Low-Energy (3 to 20 eV) Electrons. *Science* **2000**, *287*, 1658−1660.
(7) *International Comission on Radiation Units and Measurements*; IRCU Report No. 31; 1979.
(8) Aflatooni, K.; Gallup, G. A.; Burrow, P. D. Electron Attachment Energies of the DNA Bases. *J. Phys. Chem. A* **1998**, *102*, 6205−6207.
(9) Kumar, A.; Sevilla, M. D. The Role of $\pi\sigma^*$ Excited States in Electron-Induced DNA Strand Break Formation: A Time-Dependent Density Functional Theory Study. *J. Am. Chem. Soc.* **2008**, *130*, 2130−2131.
(10) Kumar, A.; Sevilla, M. D. Role of Excited States in Low-Energy Electron (LEE) Induced Strand Breaks in DNA Model Systems: Influence of Aqueous Environment. *ChemPhysChem* **2009**, *10*, 1426−1430.
(11) Probst, M.; Injan, N.; Denifl, S.; Zappa, F.; Ingo, M.; Beikircher, M.; Ptasinska, S.; Limtrakul, J.; Märk, T. D.; Mauracher, A.; Scheier, P. Calculation of Processes Relevant to Reactions between Nucleic Acids and Free Electrons. *Chem. Eng. Commun.* **2008**, *195*, 1371−1381.
(12) Ptasinska, S.; Denifl, S.; Grill, V.; Märk, T. D.; Illenberger, E.; Scheier, P. Bond- and Site-Selective Loss of H^- from Pyrimidine Bases. *Phys. Rev. Lett.* **2005**, *95*, 093201−093204.
(13) Denifl, S.; Ptasinska, S.; Hanel, G.; Gstir, B.; Probst, M.; Scheier, P.; Märk, T. D. Electron Attachment to Gas-Phase Uracil. *J. Chem. Phys.* **2004**, *120*, 6557−6565.
(14) Burrow, P. D.; Gallup, G. A.; Scheer, A. M.; Denifl, S.; Ptasinska, S.; Märk, T. D.; Scheier, P. Vibrational Feshbach Resonances in Uracil and Thymine. *J. Chem. Phys.* **2006**, *124*, 124310−124316.
(15) Scheer, A. M.; Silvernail, C.; Belot, J. A.; Aflatooni, K.; Gallup, G. A.; Burrow, P. D. Dissociative Electron Attachment to Uracil Deuterated at the N1 and N3 Positions. *Chem. Phys. Lett.* **2005**, *411*, 46−50.
(16) Scheer, A. M.; Aflatooni, K.; Gallup, G. A.; Burrow, P. D. Bond Breaking and Temporary Anion States in Uracil and Halouracils: Implications for the DNA Bases. *Phys. Rev. Lett.* **2004**, *92*, 068102−068105.
(17) Ptasinska, S.; Denifl, S.; Scheier, P.; Illenberger, E.; Märk, T. D. Bond- and Site-Selective Loss of H Atoms from Nucleobases by Very-Low-Energy Electrons (< 3 eV). *Angew. Chem., Int. Ed.* **2005**, *44*, 6941−6943.
(18) Desfrançois, C.; Periquet, V.; Bouteiller, Y.; Schermann, J. P. Valence and Dipole Binding of Electrons to Uracil. *J. Phys. Chem. A* **1998**, *102*, 1274−1278.
(19) Fermi, E.; Teller, E. The Capture of Negative Mesotrons in Matter. *Phys. Rev.* **1947**, 399−408.
(20) Crawford, O. H.; Garrett, W. R. Electron Affinities of Polar Molecules. *J. Chem. Phys.* **1977**, *66*, 4968−4970.
(21) Desfrançois, C.; Abdoul-Carime, H.; Khelifa, N.; Schermann, J. P. From $1/r$ to $1/r^2$ Potentials: Electron Exchange between Rydberg Atoms and Polar Molecules. *Phys. Rev. Lett.* **1994**, *73*, 2436−2439.
(22) Roca-Sanjuán, D.; Merchán, M.; Serrano-Andrés, L.; Rubio, M. *Ab initio* Determination of the Electron Affinities of DNA and RNA Nucleobases. *J. Chem. Phys.* **2008**, *129*, 095104−095114.
(23) Gallup, G. A.; Fabrikant, I. I. Vibrational Feshbach Resonances in Dissociative Electron Attachment to Uracil. *Phys. Rev. A* **2011**, *83*, 012706−012712.
(24) Sanche, L. Nanoscopic Aspects of Radiobiological Damage: Fragmentation Induced by Secondary Low-Energy Electrons. *Mass Spectrom. Rev.* **2002**, *21*, 349−369.
(25) Sanche, L. Interactions of Low-Energy Electrons with Atomic and Molecular Solids. *Scanning Microsc.* **1995**, *9*, 619−656.
(26) Xi, L.; Cai, Z.; Sevilla, M. D. DFT Calculations of the Electron Affinities of Nucleic Acid Bases: Dealing with Negative Electron Affinities. *J. Phys. Chem. A* **2002**, *106*, 1596−1603.
(27) Denifl, S.; Zappa, F.; Mauracher, A.; Ferreira da Silva, F.; Bacher, A.; Echt, O.; Märk, T. D.; Bohme, D. K.; Scheier, P. Dissociative Electron Attachment to DNA Bases Near Absolute Zero Temperature: Freezing Dissociation Intermediates. *ChemPhysChem* **2008**, *9*, 1387−1389.
(28) Pan, X.; Cloutier, P.; Hunting, D.; Sanche, L. Dissociative Electron Attachment to DNA. *Phys. Rev. Lett.* **2003**, *90*, 208102−208105.
(29) Li, X.; Sanche, L.; Sevilla, M. D. Low Energy Electro Interactions with Uracil: The Energetics Predicted by Theory. *J. Phys. Chem. B* **2004**, *108*, 5472−5476.
(30) Simons, J.; Jordan, K. D. Ab Initio Electronic Structure of Anions. *Chem. Rev.* **1987**, *87*, 535−555.
(31) Rubio, M.; Merchán, M.; Ortí, E.; Roos, B. O. Theoretical Study of the Electronic Spectra of the Biphenyl Cation and Anion. *J. Phys. Chem.* **1995**, *99*, 14980−14987.
(32) Pou-Amérigo, R.; Serrano-Andrés, L.; Merchán, M.; Ortí, E.; Forsberg, N. A Theoretical Determination of the Low-Lying Electronic States of the *p*-Benzosemiquinone Radical Anion. *J. Am. Chem. Soc.* **2000**, *122*, 6067−6077.
(33) Andersson, K.; Malmqvist, P.-Å.; Roos, B. O. Second-Order Perturbation Theory with a Complete Active Space Self-Consistent Field Reference Function. *J. Chem. Phys.* **1992**, *96*, 1218−1226.
(34) Serrano-Andrés, L.; Merchán, M.; Nebot-Gil, I.; Lindh, R.; Roos, B. O. Towards an Accurate Molecular Orbital Theory for Excited States: Ethene, Butadiene, and Hexatriene. *J. Chem. Phys.* **1993**, *98*, 3151−3162.
(35) Roos, B. O.; Andersson, K.; Fülscher, M. P.; Malmqvist, P.-Å.; Serrano-Andrés, L.; Pierloot, K.; Merchán, M. Multiconfigurational Perturbation Theory: Applications in Electronic Spectroscopy. In *Advances in Chemical Physics, New Methods in Computational Quantum Mechanics*, 1st ed.; Prigogine, I., Rice, S. A., Eds.; John Wiley & Sons: New York, 1996; Vol. 93, pp 219.
(36) Serrano-Andrés, L.; Merchán, M.; Borin, A. C. Adenine and 2-Aminopurine: Paradigms of Modern Theoretical Photochemistry. *Proc. Natl. Acad. Sci.* **2006**, *103*, 8691−8696.
(37) De Vico, L.; Olivucci, M.; Lindh, R. New General Tools for Constrained Geometry Optimizations. *J. Chem. Theory Comput.* **2005**, *1*, 1029−1037.
(38) Anglada, J. M.; Bofill, J. M. A Reduced-Restricted-Quasi-Newton−Raphson Method for Locating and Optimizing Energy Crossing Points between Two Potential Energy Surfaces. *J. Comput. Chem.* **1997**, *18*, 992−1003.
(39) Forsberg, N.; Malmqvist, P. Å. Multiconfiguration Perturbation Theory with Imaginary Level Shift. *Chem. Phys. Lett.* **1997**, *274*, 196−204.
(40) Karlström, G.; Lindh, R.; Malmqvist, P.-Å.; Roos, B. O.; Ryde, U.; Veryazov, V.; Widmark, P.-O.; Cossi, M.; Schimmelpfennig, B.; Neogrady, P.; Seijo, L. MOLCAS: A Program Package for Computational Chemistry. *Comput. Mater. Sci.* **2003**, *28*, 222−239.
(41) Veryazov, V.; Widmark, P.-O.; Serrano-Andrés, L.; Lindh, R.; Roos, B. O. 2MOLCAS as a Development Platform for Quantum Chemistry Software. *Int. J. Quantum Chem.* **2004**, *100*, 626−635.
(42) Periquet, V.; Moreau, A.; Carles, S.; Schermann, J.; Desfrançois, C. Cluster Size Effects upon Anion Solvation of N-Heterocyclic Molecules and Nucleic Acid Bases. *J. Electron Spectrosc. Relat. Phenom.* **2000**, *106*, 141−151.
(43) Roca-Sanjuán, D.; Merchán, M.; Serrano-Andrés, L. Modeling Hole Transfer in DNA: Low-Lying Excited States of Oxidized Cytosine Homodimer and Cytosine-Adenine Heterodimer. *Chem. Phys.* **2008**, *349*, 188−196.
(44) Serrano-Andrés, L.; Merchán, M.; Roca-Sanjuán, D.; Olaso-González, G.; Rubio, M. Bioexcimers as Precursors of Charge Transfer and Reactivity in Photobiology. *AIP Conf. Proc.* **2007**, *963*, 526−532.
(45) Roca-Sanjuán, D.; Olaso-González, G.; Coto, P. B.; Merchán, M.; Serrano-Andrés, L. Modeling Hole Transfer in DNA. II. Molecular

Basis of Charge Transport in the DNA Chain. *Theor. Chem. Acc.* **2010**, *126*, 177−183.
(46) Sponer, J.; Leszczynski, J.; Hobza, P. Electron Properties, Hydrogen Bonding, Stacking, and Cation Binding of DNA and RNA Nucleobases. *Biopolymers* **2001**, *61*, 3−31.
(47) Svozil, D.; Jungwirth, P.; Havlas, Z. Electron Binding to Nucleic Acid Bases. Experimental and Theoretical Studies. A Review. *Collect. Czech. Chem. Commun.* **2004**, *69*, 1395−1428.